Evidence for Macroscopic Quantum Tunneling of Phase Slips in Long One-Dimensional Superconducting Al Wires

Fabio Altomare,[1,*] A. M. Chang,[1,*] Michael R. Melloch,[2] Yuguang Hong,[3] and Charles W. Tu[3]

[1]*Physics Department, Purdue University, West Lafayette, Indiana 47906, USA and Department of Physics, Duke University, Durham, North Carolina 27708, USA*

[2]*School of Electrical and Computer Engineering, Purdue University, West Lafayette, Indiana 47906, USA*

[3]*Department of Computer and Electrical Engineering, University of California at San Diego, La Jolla, California 92093, USA*

(Received 31 May 2005; published 6 July 2006)

Quantum phase slips have received much attention due to their relevance to superfluids in reduced dimensions and to models of cosmic string production in the early universe. Their establishment in one-dimensional superconductors has remained controversial. Here we study the nonlinear current-voltage characteristics and linear resistance in long superconducting Al wires with lateral dimensions ~5 nm. We find that, in a magnetic field and at temperatures well below the superconducting transition, the observed behaviors can be described by the nonclassical, macroscopic quantum tunneling of phase slips, and are inconsistent with the thermal activation of phase slips.

DOI: 10.1103/PhysRevLett.97.017001 PACS numbers: 74.78.Na, 74.25.Fy, 74.25.Ha, 74.40.+k

What is the resistance of a superconductor below its superconducting transition temperature? For a three-dimensional superconductor, the answer is the obvious one—zero. But in one dimension, by which we mean very thin very long wires, quantum fluctuations destroy the zero resistance state. Phase slips—small superconducting regions that become normal, allowing the phase of the order parameter to rapidly change by 2π—give rise to residual resistance and can even quench superconductivity completely. The tiny cross section of 1D nanowires reduces the free-energy barrier arising from a loss of condensation energy in the creation of phase slips. Thermal activation of phase slips (TAPS) across this barrier is responsible for the residual resistance just below T_c (LAMH picture) [1]. On the other hand, macroscopic quantum tunneling of phase slips (QTPS) as the source of residual resistance at low temperatures has remained controversial despite intense experimental effort [2–8]. The observation of macroscopic quantum tunneling is of significance not only for 1D superconductivity, but also for understanding the decoherence of quantum systems due to interaction with their environment. Here we clearly establish the presence of QTPS in superconducting (SC) Al nanowires, showing the dramatic effect they have on the current-voltage (I-V) characteristics of the wire.

Phase slips in 1D SC nanowires have traditionally been studied by measuring the linear resistance as a function of the temperature through the normal-superconducting (NS) transition. Any resistance in excess to that predicted by thermal activation is attributed to macroscopic tunneling of phase slips [2–7]. However, this attribution can be flawed because of weak links in the wire resulting from inhomogeneities [3,7]. Moreover, the fitting of the excess residual resistance to quantum-phase-slip expressions [2,5–7] often necessitated an *ad hoc* reduction in the free-energy barrier. Recently Rogachev *et al.* [8] examined the nonlinear I-V dependence of $Mo_{0.79}Ge_{0.21}$ SC nanowires: they found that the deduced residual resistance, spanning 11 orders in magnitude, followed the prediction of classical TAPS alone, thus contradicting previous claims of QTPS behavior based on residual linear resistance by the same group [4,5].

In this Letter, we examine the nonlinear I-V characteristics and linear resistance of long Al nanowires, the narrowest one with dimension 5.2 nm × 6.1 nm × 100 μm (21 × 24 × 400 000 atoms). Our wires are much longer than those of similar cross section reported in the literature (~0.5 μm long) [4,5,8] and the ratio of the low temperature SC coherence length to the width (or height) is also much larger, thus placing us in a regime distinct from previous works. Specifically, we study the residual resistance deduced from the nonlinear I-V characteristics in the superconducting state below the critical current. Our main finding is that the I-V dependence and residual resistance are inconsistent with the classical LAMH behavior, but instead are well described by quantum expressions, either derived from an extension of the classical model [2] or in a recently proposed power-law form [9–11]. The good fits to the different quantum expressions, which closely overlap each other, are corroborated by measured residual linear resistance, achieving full consistency within the quantum scenario using a single set of fitting parameters. Our results demonstrate the importance of nonclassical, quantum phase slips in ultranarrow, 1D superconducting aluminum wires.

The nanowires were fabricated by thermally evaporating aluminum onto a narrow, 8 nm-wide, molecular-beam epitaxy (MBE) grown InP ridge, while at once linking and partially covering the four-terminal Au/Ti measurement pads [Fig. 1(b)]. The fabrication is described elsewhere [12]. Magnetoresistance at 4.2 K (above T_c) was used to characterize the wires (Table I). The calculated dirty limit ξ [13] (≈94 nm for s1, ≈128 nm for s2) far exceeds the lateral dimensions (~5–9 nm).

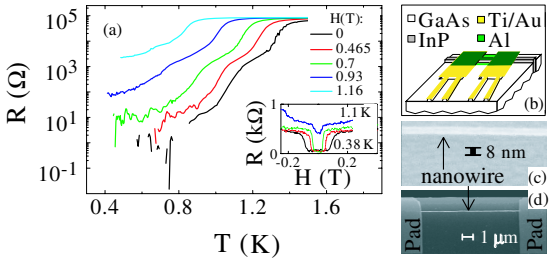

FIG. 1 (color online). (a) Linear resistance versus temperature for wire s2 in different magnetic fields; the pad series resistance has been subtracted [15]. Inset: The pad series resistance increases at magnetic fields beyond the critical field of the pad regions covered by aluminum ($T = 0.38, 0.80, 0.99, 1.10$ K). (b)–(d) Schematic and scanning electron microscopy (SEM) images of a nominally 8-nm wide Al nanowire (similar to samples s1 and s2): the Al layer does not entirely cover the Au/Ti pads which were measured in series with the superconducting wire.

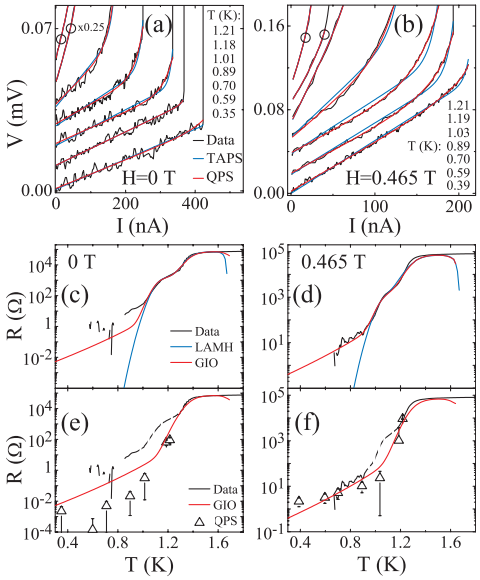

FIG. 2 (color). Nonlinear I-V curves and linear resistance for sample s2 at different magnetic fields (H): Black curves–data; red curves–fits to the GIO (≡ GIO + LAMH) expressions for QPS (≡ TAPS + QTPS), and blue curves—fits to the LAMH expressions for TAPS alone. (a)–(b) I-V curves offset for clarity. The fits to QPS are of higher quality compared to TAPS; each fit includes a series resistance term V_S. These I-V curves can be fitted equally well by a power-law form $V = V_S + K \cdot (I/I_k)^\nu$ where $12 \gtrsim \nu \gtrsim 3.2$ for $0 \le H \le 1.05$ T [10,11]. (c)–(d) Linear resistance after background subtraction [see Fig. 1(a) and [15]]. The LAMH fits are poor at low T. (e)–(f) The resistance contribution due to phase slips ($R_{\rm QPS}$) extracted in (a)–(b) from fits to the I-V curves using the GIO expressions (discrete points, △). $R_{\rm QPS}$ and the linear resistance from (c)–(d) are refitted using the GIO expressions (red) with the same $a_{\rm GIO}(= 1.2)$ while disregarding the irrelevant shoulder feature (dashed line).

To investigate the SC behavior, the linear resistance through the NS transition was measured at a current of 1.6 nA [Fig. 1(a)], while the nonlinear I-V characteristics were measured in both the constant-current [Figs. 2(a), 2(b), and 3] and constant-voltage modes below T_c [14]. The linear resistance drops by several orders of magnitude from the normal state resistance (R_N) through T_c, but remains finite. In Fig. 1(a) we show the linear resistance versus temperature for wire s2 in different magnetic fields (H) [15]. At a given temperature, the resistance increases with increasing H as superconductivity weakens. In the constant-current mode, finite residual nonlinear voltage is observed in the I-V curves below the critical current jump. Such residual voltage is unobservable in large wires. In the constant-voltage mode, the I-V curves exhibit nonhysteretic voltage steps and S-shaped curves down to $T/T_c \approx 0.2$, typical of 1D superconductors [6,16]. Evidences for wire homogeneity include: (1) comparable critical current density in wires s1 and s2, (2) all I-V traces in the constant-current mode showed a single critical current jump.

To assess the importance of QTPS, we focus on the residual resistance and residual voltage below T_c for sample s2; the wider s1 will be used for control as discussed below. The main data sets consist of the nonlinear I-V curves in constant-current mode [Figs. 2(a), 2(b), and 3 (black curves)], and the linear resistance versus T. This latter resistance is obtained in two ways: (i) from the data in Fig. 1(a) [15] [Figs. 2(c) and 2(d) (black curves)], and (ii) from the fits to the nonlinear I-V curves according to Eqs. (1b) and (3) below (△, Figs. 2(e) and 2(f)). It will be demonstrated through quantitative analysis that this entire set of data is inconsistent with the TAPS scenario, as evidenced by the poor fits to the LAMH expressions [Eqs. (1a) and (1b)] shown in Figs. 2 and 3 (blue curves). Instead, the inclusion of the QTPS contributions [Giordano (GIO) model Eqs. (2) and (3)] in the fits is essential in providing a fully consistent description based on a single set of parameters (see red curves in Figs. 2 and 3).

Thermal activation of phase slips, important at $T \lesssim T_c$, is well described by the expressions derived by Langer, Ambegaokar, McCumber, Halperin (LAMH) [1,17]:

TABLE I. Parameters for sample s1 and s2, including L (length), w (width), t (thickness), R_N (normal state resistance), ρ (resistivity), l_e (mean free path), ξ (GL coherence length), and J_c (critical current density). w, t, ρ, and l_e were deduced based on magnetoresistance measurements [12]. ξ was calculated using $\xi = 0.85\sqrt{\xi_0 l_e}$, where $\xi_0 = 1600$ nm is the GL superconducting coherence length in bulk aluminum.

	L μm	w nm	t nm	R_N kΩ	ρ μΩ cm	l_e nm	ξ nm	$J_c(0.35\ \text{K})10^5$ A/cm^2
s1	10	6.9	9.0	8.3	5.1	7.6	94	12.1
s2	100	5.25	6.09	86	2.8	14.3	128	13.1

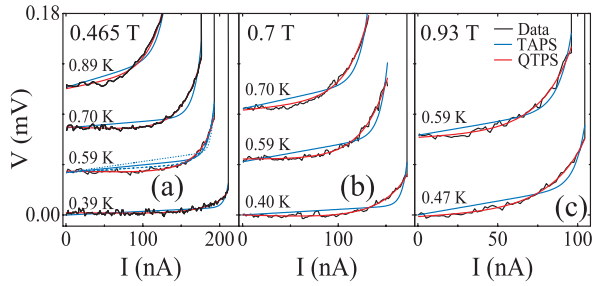

FIG. 3 (color). The nonlinear I-V curves, at $T/T_c \lesssim 0.5$ are refitted with $V = V_{\mathrm{QTPS}} + V_S$ and $V = V_{\mathrm{TAPS}} + V_S$ (see text). (a)–(c) The data (black), QTPS (red), and TAPS (blue) fits are shown after subtracting the linear background. Dotted (dashed) line in (a) is the fit to the TAPS expression with a 50% reduction (increase) in temperature, respectively.

$$R_{\mathrm{LAMH}} = R_q \frac{\Omega}{k_B T} \exp\left(-\frac{\Delta F}{k_B T}\right), \tag{1a}$$

$$V_{\mathrm{TAPS}} = I_0 R_{\mathrm{LAMH}} \sinh(I/I_0), \tag{1b}$$

where the quantum resistance $R_q = \pi\hbar/2e^2$, attempt frequency $\Omega = (L/\xi)(\Delta F/k_B T)^{1/2}(\hbar/\tau_{\mathrm{GL}})$, free-energy barrier $\Delta F = (8\sqrt{2}/3)(H_{\mathrm{th}}^2/8\pi)A\xi$, and the Ginzburg-Landau relaxation time $\tau_{\mathrm{GL}} = (\pi/8)[\hbar/k_B(T - T_c)]$, $I_0 = 4ek_BT/h$. L is the wire length, T the temperature, k_B the Boltzmann constant, H_{th} the thermodynamical critical field, A the wire cross section, and ξ the GL coherence length.

Quantum tunneling of phase slips, which takes place in parallel with thermal activation, is expected to dominate at low T. Giordano [2] proposed a quantum form by replacing kT with $(1/a_{\mathrm{GIO}})(\hbar/\tau_{\mathrm{GL}})$ [17,18]:

$$R_{\mathrm{GIO}} = R_q \frac{L}{\xi} \sqrt{a_{\mathrm{GIO}} \frac{\Delta F}{\hbar/\tau_{\mathrm{GL}}}} \exp\left(-a_{\mathrm{GIO}} \frac{\Delta F}{\hbar/\tau_{\mathrm{GL}}}\right), \tag{2}$$

where a_{GIO} is a numerical constant of order unity and, in analogy with the thermal case, we propose that [17,18]:

$$V_{\mathrm{QTPS}} = I_{\mathrm{GIO}} R_{\mathrm{GIO}} \sinh(I/I_{\mathrm{GIO}}), \tag{3}$$

where $I_{\mathrm{GIO}} = 2e/(\pi\tau_{\mathrm{GL}} a_{\mathrm{GIO}})$. In this quantum case, a resistance similar to the Giordano expression (and numerically equivalent) has been recently derived, on a microscopic basis, by Golubev and Zaikin [9] and by Khlebnikov and Pryadko [10]. In the nonlinear regime, both theories predict a crossover from an exponential dependence to a power-law behavior ($V \propto I^{\nu}$) at low T.

To begin the analysis, we first extract the parameters, T_c and ξ at each magnetic field and a single a_{GIO}, by fitting to the linear R versus T traces in Figs. 2(c) and 2(d); T_c and a_{GIO} are input parameters in the analysis of the I-V curves. Below T_c, a wire is modeled as a normal and a superconducting wire in parallel, the latter with a resistance produced by the relevant phase slips mechanism [5]. To account for the shoulder feature at a resistance $\approx 1/20$ of R_N, we assume our wire to be composed of segments of two slightly different cross sectional areas, with a fixed ratio of 90% ($\Delta F \propto A$). The thinner segments corresponding to the smaller cross sectional area have a larger T_c [7]. These segments, with critical temperature (resistance) T_{c1} (R_1), are responsible for $\gtrsim 95\%$ of R_N. At zero field, the fitting parameters are $T_{c1}(H = 0)$, $T_{c2}(H = 0)$, $\xi(H = 0)$, R_1, and a_{GIO}, while at $H \geq 0.465$ T, only $T_{c1}(H)$, $T_{c2}(H)$, $\xi(H)$ are varied. Fitting using two ξs produced unphysical ξ dependence on H and was discarded. The fits to the GIO (red) and LAMH (blue) theory are presented in Figs. 2(c) and 2(d). At $H = 0$ T both fits reproduced the data over several decades in resistance and are nearly equivalent above $\approx 5\ \Omega$. At higher field the GIO theory better models the data, particularly at low T [19]. The fitting parameters T_{c1} and ξ (○) are presented in Fig. 4(a) and 4(b). Their H dependence can be fitted to simple theoretical expressions as shown. The single value of $a_{\mathrm{GIO}} = 1.2$ we obtain, of order unity as expected, will be used throughout all the subsequent analysis.

Despite the success in fitting to the linear resistance, it is not possible to completely rule out weak links as the source of residual resistance. To clearly demonstrate the importance of quantum phase slips, it is necessary to analyze the nonlinear I-V dependence. Generalizing the nonlinear analysis of Rogachev *et al.* [8] by including QTPS while also accounting for series resistances, the total voltage drop across the superconducting nanowire is $V = V_{\mathrm{TAPS}} + V_{\mathrm{QTPS}} + V_S$, where V_{TAPS} and V_{QTPS} are given in Eqs. (1b) and (3), respectively [17], and $V_S = R_S I$. R_S is a series resistance which includes the contribution of the pads and other Ohmic-like contributions such as proximity effect of the normal pads on the SC wire [20]. The fitting parameters are R_{TAPS}, R_{QTPS}, and R_S [17], while $a_{\mathrm{GIO}}(= 1.2)$ and $T_c(H)$, which enters through τ_{GL}, are taken from the previous fits [Fig. 4(a)]. At all temperatures and fields, the fitting curves reproduce the data extremely well, as

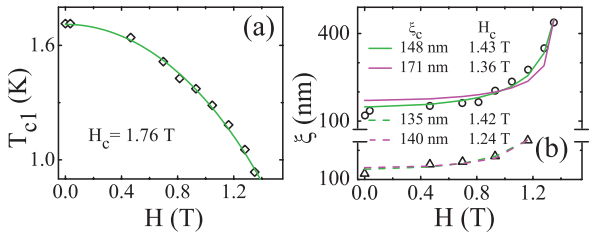

FIG. 4 (color). GIO(≡ GIO + LAMH) fitting parameters to the linear resistance curves, including those shown in Fig. 2(c) and 2(d), plotted versus H. (a) T_{c1} (◇) and T_{c2} (not shown) fit well to the pair breaking perturbation theory [13] (green). (b) ξ (○) is fitted to both $\xi = \xi_c/\sqrt[4]{1 - (H/H_c)^2}$ (magenta) [$\Delta \propto \sqrt{1 - (H/H_c)^2}$ and $\xi \propto 1/\sqrt{\Delta}$ [13]], and to an *ad hoc* expression $\xi = \xi_c/\sqrt{1 - (H/H_c)^2}$ (green); $\xi_c \equiv \xi(H = 0)$ and H_c is the critical field. ξ is better described by the *ad hoc* expression. ξ (△) derived from the fits to R_{QPS}, including those in Fig. 2(e) and 2(f), is fitted to theory as before (dashed lines) yielding $\xi_c \approx$ 135 nm, within 5% of the value in Table I.

shown in red in Figs. 2(a), 2(b), and 3 [21]. At higher T ($T/T_c \gtrsim 0.7$) the contribution from QTPS is negligible compared to TAPS. At low T ($T/T_c \lesssim 0.5$) TAPS is expected to be exponentially suppressed [Eq. (1a)] and QTPS should dominate; this expectation is confirmed by the fits which yielded a negligible R_{TAPS} compared to R_{QTPS} [22].

To further substantiate the importance of QTPS at low T while at the same time rule out TAPS as a significant cause of phase slips, we directly compare fits of the nonlinear I-V curves using $V = V_{\mathrm{QTPS}} + V_S$ and $V = V_{\mathrm{TAPS}} + V_S$. The fitting parameters for QTPS are R_{QTPS}, R_s, and for TAPS they are R_{TAPS}, R_S. The curves are presented in Figs. 3(a)–3(c) after subtracting the linear background for several $H > 0$ T. Although the two expressions have the same number of parameters, the QTPS fits (red) are of good quality while the TAPS fits (blue) are evidently much poorer. Varying T by $\pm 50\%$ in the TAPS fits still failed to reproduce the data, as shown in Fig. 3(a) for $T = 0.59$ K and $H = 0.465$ T. Comparing the χ squares of the fits that include QTPS versus TAPS alone using the statistical F test yielded strong support for the importance of quantum phase slips with a confidence level $>99.99\%$ [23].

The $R_{\mathrm{QPS}} = R_{\mathrm{QTPS}} + R_{\mathrm{TAPS}}$ extracted from the nonlinear I-V fits enables to exclude contributions to residual resistance that are irrelevant to phase slips, providing a means to check full consistency. In Figs. 2(e) and 2(f) we plot R_{QPS} ($\triangle$ symbols) for $T \lesssim T_c$ and replot the linear resistance through the NS transition for comparison; we then refit the linear resistance expressions [GIO + LAMH, Eqs. (1a) and (2)] to these data, keeping $a_{\mathrm{GIO}} = 1.2$ unaltered while varying T_c and ξ. The discrete R_{QPS} data points versus T no longer exhibit a shoulder feature, and only one T_c was needed. Satisfactory agreement is achieved as depicted in Figs. 2(e) and 2(f) (red). Similar agreement comparable to the $H = 0.465$ T trace is obtained at higher $H = 0.7$ T, 0.93 T, etc. T_c was essentially unchanged compared to T_{c1} in Fig. 4(a) but ξ [Fig. 4(b), $\triangle$] was reduced at higher H, compared to the data obtained previously [Fig. 4(b), $\bigcirc$). Fitting to the new values yielded $\xi_c \equiv \xi(H = 0) \approx 135$ nm, within 5% of the calculated value in Table I. As a final consistency check, analysis of the wider superconducting sample s1 [12] did not produce any sign of QTPS for $H \lesssim 0.9$ T. This is sensible because of the larger free-energy barrier.

The consistency achieved in our analysis of the nonlinear I-V curves and residual resistance, supported by the quantitative statistical F test, demonstrates the importance of quantum phase slips. This helps rule out other scenarios, e.g., TAPS alone or weak links. Furthermore, our results establish that the transport properties of 1D superconducting nanowires at temperatures much below T_c are determined primarily by the macroscopic quantum tunneling of phase slips. Our findings pave the way to the study of newly predicted quantum phase transitions in metallic nanowires [24].

F. A. thanks M. E. Rizza for her support. Work supported by NSF No. DMR-0135931 and No. DMR-0401648.

*Present address: Physics Department, Duke University, Durham, North Carolina 27708, USA.

[1] J. S. Langer and V. Ambegaokar, Phys. Rev. **164**, 498 (1967); D. E. McCumber and B. I. Halperin, Phys. Rev. B **1**, 1054 (1970).
[2] N. Giordano, Phys. Rev. Lett. **61**, 2137 (1988).
[3] J. M. Duan, Phys. Rev. Lett. **74**, 5128 (1995).
[4] A. Bezryadin *et al.*, Nature (London) **404**, 971 (2000).
[5] C. N. Lau *et al.*, Phys. Rev. Lett. **87**, 217003 (2001).
[6] M. L. Tian *et al.*, Phys. Rev. B **71**, 104521 (2005).
[7] M. Savolainen *et al.*, Appl. Phys. A: Mater. Sci. Process. **79**, 1769 (2004); M. Zgirski *et al.*, Nano Lett. **5**, 1029 (2005).
[8] A. Rogachev *et al.*, Phys. Rev. Lett. **94**, 017004 (2005).
[9] D. S. Golubev and A. D. Zaikin, Phys. Rev. B **64**, 014504 (2001).
[10] S. Khlebnikov and L. P. Pryadko, Phys. Rev. Lett. **95**, 107007 (2005).
[11] See EPAPS Document No. E-PRLTAO-97-038627 for details of the proposed power-law dependence (Sec. 1). For more information on EPAPS, see http://www.aip.org/pubservs/epaps.html.
[12] F. Altomare *et al.*, Appl. Phys. Lett. **86**, 172501 (2005).
[13] M. Tinkham, Introduction to Superconductivity (McGraw-Hill, New York, 1996).
[14] Linear resistance measurements were performed with a lock-in amplifier at 23 Hz. Room temperature filters and low temperature RC filters, formed naturally from the sample lead resistances ($\approx$2–20 kΩ) and capacitances to ground ($\approx$0.5 nF), helped reduce noise to the nanowires.
[15] See EPAPS Document No. E-PRLTAO-97-038627 for details of the subtraction of the series resistance (Sec. 2). For more information on EPAPS, see http://www.aip.org/pubservs/epaps.html.
[16] D. Y. Vodolazov *et al.*, Phys. Rev. Lett. **91**, 157001 (2003).
[17] To distinguish the fitting parameters from the theoretical values, we refer to R_{TAPS} (R_{QTPS}) as the TAPS (QTPS) resistance extracted from fits to the V, I, and to R_{LAMH} (R_{GIO}) as the calculated values for TAPS (QTPS).
[18] In the following, when referring to the GIO theory, we will implicitly include the LAMH contribution as well.
[19] At sufficiently high H field, the rapid increase in ξ and decrease in T_{c1} reduces the free-energy barrier $[\Delta F(H,T) \approx 0.83 \frac{R_q}{R_N} \frac{L}{\xi(H,T=0)} k_B T_{c1}(H)(1 - T/T_{c1}(H)]^{3/2}$ [6] [Fig. 4(a) and 4(b)]. For a *given intermediate temperature* the contribution from TAPS can actually become larger.
[20] G. R. Boogaard *et al.*, Phys. Rev. B **69**, 220503(R) (2004).
[21] See EPAPS Document No. E-PRLTAO-97-038627 for the establishment of the nanowire electron temperature (Sect. 4). For more information on EPAPS, see http://www.aip.org/pubservs/epaps.html.
[22] For the data central to QTPS shown in Figs. 2(f) and 3, there were a total of 21 fitting parameters for 1106 data points in the 10 traces, or 53 points per parameter.
[23] See EPAPS Document No. E-PRLTAO-97-038627 for details of the F test (Sec. 3). For more information on EPAPS, see http://www.aip.org/pubservs/epaps.html.
[24] S. Sachdev *et al.*, Phys. Rev. Lett. **92**, 237003 (2004).